Environ Earth Sci (2017) 76:592
DOI 10.1007/s12665-017-6913-1

ORIGINAL ARTICLE

Longitudinal dispersion in an open channel determined from a tracer study

Tomáš Julínek[1] · **Jaromír Říha**[1]

Received: 5 April 2017 / Accepted: 14 August 2017 / Published online: 28 August 2017

Abstract The modelling of pollution transport processes in open channels requires good knowledge about parameters such as hydrodynamic dispersion, advection and decay rates. These parameters can be determined by tracer studies. The basic output of these studies takes the form of observed time course data for the concentration of injected tracer in sampling profiles. In this study, Rhodamine WT fluorescein dye was used as a tracer. The travel time of the front and tail of the dye cloud and the magnitude of the peak concentration can be additionally derived. Two dye tests were carried out at the Svitava and Svratka rivers in the Czech Republic. These are rivers which are mostly regulated and feature widths ranging from 10 to 25 m. Data were collected from 4 and 5 sampling profiles, respectively, along 16.1-km-long reaches of the rivers. The transport parameters were derived via inverse numerical analysis of the collected data and were compared with values obtained by previously published empirical formulas based on dimensional analysis. The resulting dispersion coefficient was from 7.2 to 9.5 m^2/s and showed good agreement with previous studies.

Keywords Pollution transport · Hydrodynamic dispersion · Dye test · Modelling

List of symbols

a	Dispersion factor (m)
A	Flow area (m^2)
c	Concentration (kg/m^3)
C	Chezy´s coefficient ($m^{0,5}/s$)
D_L	Longitudinal hydrodynamic dispersion (dispersion coefficient) (m^2/s)
E_Q, E_c	Efficiency coefficients of hydrological and transport models (-)
g	Gravitational acceleration (m/s^2)
h	Cross-sectional average water depth (m)
H	Water level (m)
L_M	Mixing length (m)
Q	Discharge (m^3/s)
R	Hydraulic radius (m)
s	Source/sink per reach length (kg/s)
t	Time (s)
u	Mean profile velocity (m/s)
u^*	Shear velocity (m/s)
V	Volume change of matter ($kg/s/m^3$)
w	Channel width at water surface (m)
x	Spatial coordinate along the centre line of the channel (m)
β	Boussinesq number (-)

Introduction

Stream water quality modelling is broadly used to assess current conditions and the impacts of proposed measures within stream water quality management. For such modelling, it is essential to have data on parameters describing transport processes such as hydrodynamic dispersion,

Electronic supplementary material The online version of this article (doi:10.1007/s12665-017-6913-1) contains supplementary material, which is available to authorized users.

✉ Tomáš Julínek
julinek.t@fce.vutbr.cz

[1] Faculty of Civil Engineering, Institute of Water Structures, Brno University of Technology, Brno, Czech Republic

advection and decay rates. To that end, both laboratory and field tracer experiments are performed so as to quantify those parameters. Additional to the advection phenomena, which can be described by standard hydrodynamics, dispersion plays a significant role in pollution transport in rivers. Even if various empirical and other numerical methods may be applied to the determination of dispersion parameters (namely the coefficient of dispersion), tracer experiments carried out at watercourses are of key importance in the quantification of dispersion characteristics. One of the most used and suitable quantitative tracers are dyes, namely fluoresceins (Feuerstein and Selleck 1963; Flury and Wai 2003). As Rhodamine WT fluorescein dye tracer was used in this study, the term "dye test" is used throughout the following text.

In this study, two dye tests using Rhodamine WT fluorescein tracer were carried out in the city of Brno (Czech Republic) at the Svitava and Svratka rivers, which are medium size regulated rivers. The dye concentration was identified (traced) in five profiles along the channels using a Turner 10-AU fluorometer. The dispersion phenomenon in moving bodies of water is expressed by the dispersion factor a and the coefficient of longitudinal dispersion D_L, which was determined by an inverse procedure carried out via the calibration of a numerical model. To obtain results that are more reproducible, the obtained coefficients of longitudinal dispersion were related to the geometric and hydraulic characteristics of the streams and compared to empirical formulas published in the literature.

The determined hydrodynamic dispersion values were subsequently applied during the development of the Brno city water management plan for the evaluation of the impact of proposed measures on the sewerage system, namely the proposed capacity of reconstructed and newly built storm water overflows and retention chambers.

Literature review

The transport of matter has been subject to numerous studies dealing with a wide range of particular problems like hydrological modelling, the determination of dispersion characteristics, tracer applications, etc.

Hydrological modelling, including the modelling of open channel hydraulics and the transport of solids, has been a well-established discipline since the 1970s (Yotsukura and Fiering 1964; Abbot and Cunge 1982; Ambrose et al. 1994), when demands for the computer-based forecasting of stream water quality were driven by environmental legislation. Numerous user-friendly computer codes (Brown and Barnwell 1987; Crowder et al. 2004; DHI 2016; HEC-RAS 2016) using various numerical methods, such as the finite difference method, the method of characteristics and others, have recently become available for the efficient modelling of flow and pollution transport in open channels. In the case of river systems, one-dimensional (1D) models are frequently applied. Such models have also been applied as part of warning systems (Leibundgut et al. 1993) or for the evaluation of the influence of point sources of pollution such as storm water overflows. Approaches to modelling the process of advection–dispersion also include analytical solutions of the advection–dispersion equation (Van Genuchten and Alves 1982; Daněček et al. 2002) under simplified hydrodynamic conditions (e.g. during uniform channel flow).

The reliability of numerical models primarily depends on the input parameters, which include characteristics like the geometry of channels and hydraulic structures, channel roughness and transport characteristics, of which the most influential is hydrodynamic dispersion. Also very important is the apposite implementation of initial and boundary conditions. Even if the values of the mentioned parameters may be determined using various predictive techniques like genetic programming (Riahi-Madvar et al. 2009; Azamathulla and Wu 2011) or empirical formulas, the most reliable technique is considered to be backward analysis via the calibration of numerical models (Ani et al. 2009) using data from tracer studies.

The following discussion deals with the coefficient of longitudinal dispersion. The different characteristics of open channels influence the longitudinal dispersion coefficient (Toprak et al. 2004). Most of the empirical formulas for the determination of the coefficient of longitudinal dispersion are based on Eq. (11), which was introduced by Fisher et al. (1967, 1979), taking into account the geometrical and friction properties of the channel. With respect to the particular hydrodynamic and geometrical characteristics of a stream, modified equations were proposed by Liu (1977) and Seo and Cheong (1998). Deng et al. (2001) implemented the local mixing coefficient into the original Eq. (11). Vegetation along the banks in the riparian zone may significantly influence the longitudinal dispersion and transport of pollutants. Murphy et al. (2007), Perucca et al. (2009) and Tealdi et al. (2010) show the importance of vegetation, having found that mean velocity in channels with vegetation can differ significantly from that found in non-vegetated channels.

Numerous authors have derived their formulas for the determination of dispersion characteristics based on the results of tracer experiments carried out since the 1960s on artificial channels in laboratories, as well as on natural streams (Tayfur and Singh 2005). Kashefipour and Falconer (2002) published an equation derived through the application of statistical and regression analysis to previously published data.

Tracer experiments have been carried out in open channels of various sizes to derive longitudinal dispersion coefficients and verify empirical formulas (Veliskova and Kohutiar 1992; Leibundgut et al. 1993; Van Mazijk and Veling 2005; Kim 2012). Evaluation of the longitudinal dispersion coefficient by inverse analysis is usually based on the modelling of the advection–dispersion process (van Mazijk 1996; Martin et al. 1999; Boxall and Guymer 2007; Sahay 2013). Attempts to use inverse modelling and genetic algorithms, and to apply neural networks, were made by Sahay (2011) and Ani et al. (2009).

A variety of tracers may be applied during experiments (Pujol and Sanchez-Cabeza 1999; Field 2003). Tracers should fulfil certain requirements such as high solubility in water, easy detection, low background concentration in natural streams, conservative behaviour, negligible impact on the aquatic environment and low cost. From this perspective, fluorescent dyes are the most suitable and most frequently used tracers (Feuerstein and Selleck 1963; Flury and Wai 2003). They include Fluorescein, Lissamine FF, Rhodamine B and Rhodamine WT (McCutcheon 1989). Rhodamine WT is commonly used as a dye tracer as its properties meet the aforementioned requirements well (Martin et al. 1999; USEPA 1989). Therefore, Rhodamine WT was selected for the study described in this paper.

Methods

Theoretical considerations

The solution concerns two separate problems, namely open channel flow and solute transport. Traditionally, the problems are treated as one-dimensional (Ambrose et al. 1994; van Mazijk 1996). For a 1D open channel flow, the following holds (Abbot and Cunge 1982; Jain 2000):

$$\text{Mass conservation } \frac{\partial A}{\partial t}+\frac{\partial Q}{\partial x}=q \tag{1}$$

$$\text{Momentum conservation } \frac{\partial Q}{\partial t}+\frac{\partial\left(\beta\frac{Q^2}{A}\right)}{\partial x}+gA\frac{\partial H}{\partial x}+\frac{gQ|Q|}{C^2AR}=0 \tag{2}$$

where Q is discharge, A is the flow area, q is lateral inflow, H is water level, C is Chezy's velocity coefficient, R is hydraulic radius, g is gravitational acceleration, and β is the Boussinesq number.

Initial conditions express the discharge and water level at the beginning of the solution (t_0):

$$Q(x,t_0)=Q_0(x); H(x,t_0)=H_0(x) \tag{3}$$

At the upstream boundary profiles time varying values of H and Q are specified.

$$H(0,t)=\bar{H}(t); Q(0,t)=\bar{Q}(t), \tag{4}$$

where $\bar{H}(t)$and $\bar{Q}(t)$ are the known water level and discharge. The downstream boundary is defined by the rating curve (*Q-H)*.

Transport processes in open channels are described by the convection–diffusion equation (Fourier 1822; Fischer 1967; Fischer et al. 1979; Knopman and Voss 1987):

$$\frac{\partial c}{\partial t}+u\frac{\partial c}{\partial x}-D_L\frac{\partial^2 c}{\partial x^2}=V+\frac{1}{A}\frac{\partial s}{\partial x}; u=\frac{Q}{A}, \tag{5}$$

where c is solute concentration, u is cross-sectional mean velocity, D_{L} is longitudinal hydrodynamic dispersion (dispersion coefficient) including molecular diffusion and namely the effects of the variation of local velocity across the flow profile, V is the volume change of matter (e.g. retardation), s is source/sink per reach length, t is time, and x is a spatial coordinate along the centre line of the channel.

The initial condition expresses the concentration at time $t_0 = 0$,

$$c(x,t_0)=c_0(x). \tag{6}$$

Boundary conditions are prescribed concentrations in the upstream profile of studied domain $x = 0$:

$$c(0,t)=\bar{c}(t), \tag{7}$$

where $\bar{c}(t)$ is the known concentration.

A zero concentration gradient is applied in the downstream boundary profile $x = L$,

$$\frac{\partial c(L,t)}{\partial x}=0. \tag{8}$$

In Eq. (5), the key parameters are flow velocity $u(x, t)$ and coefficient D_{L}, both of which generally change over time and along the stream. The flow velocity $u(x, t)$ is determined by a hydrodynamic model (Crabtree et al. 1996) specified by Eqs. (1)–(4).

The longitudinal dispersion coefficient is related to the hydraulic and geometric characteristics of a given open channel, and also to fluid properties (Seo and Cheong 1998):

$$D_{\mathrm{L}}=f(\rho,\upsilon,u,u^*,w,h) \tag{9}$$

where ρ and v are fluid density and viscosity. The hydraulic characteristics are velocity u and shear velocity u*, and the geometric characteristics are width w and water depth h.

Dimensional analysis defines the relationship between the longitudinal dispersion coefficient and the above-mentioned characteristics. The influence of the fluid properties in a natural stream is practically negligible (Seo and Cheong 1998). In such streams the friction losses and all channel irregularities like contractions, expansions, etc., may be included in the shear velocity term. Based on these

assumptions, Eq. (9) may be rewritten in dimensionless form:

$$D_{\mathrm{L}} = f\left(\frac{u}{u^*}, \frac{w}{h}\right) \tag{10}$$

Relation (10) has been taken into account by various authors, who have expressed the longitudinal dispersion coefficient via empirical equations based on the results of laboratory and field measurements (Table 1).

In Table 1, u is the mean velocity, w is channel width, h is water depth, ε_T is the lateral mixing coefficient, and u^* is shear velocity:

$$u^* = (g.h.J_E)^{0.5} \tag{17}$$

where J_E is the energy line slope. Substituting

$$J_E = \frac{u^2}{C^2 h} \tag{18}$$

from the Manning's equation into Eq. (17) results (after some manipulation) in:

$$u^* = \frac{\sqrt{g}}{C}.u \tag{19}$$

In this study the longitudinal dispersion coefficient D_{L} was expressed by the formula:

$$D_{\mathrm{L}} = a.u \tag{20}$$

implemented in the MIKE 11 computer code (DHI 2016). Here, a is the dispersion factor (a parameter which has to be calibrated) taking into account the geometrical and frictional parameters of the channel.

Using Eqs. (17)–(19), formulas (11)–(16) were rearranged in Table 2 to formally satisfy Eq. (20).

Backward analysis

In this study, the dispersion factor a was quantified via a backward analysis of the dye test (see The dye tests, Results sections). The experimentally derived values a and D_{L} were compared with results obtained using Eqs. (20)–(26).

The solution involved the setup and calibration of both the hydrodynamic and the solute transport model. The calibration dataset consisted of a time series of measured discharges and dye concentrations. The analysis utilised the unsteady 1D hydrodynamic and convection–dispersion model of a conservative solute (Eqs. (1)–(8)) using MIKE 11 computer code.

First, the calibration of the hydrodynamic model was carried out. The boundary conditions were defined as discharge time series in upstream profiles at gauging stations G1 and G2 (Fig. 1). The initial conditions were defined as the observed discharge and water depth along the reaches at time $t_0 = 0$. The calibration and validation dataset represented discharges during Test I and Test II. The discharges in the Svitava River were approximately constant, while in the Svratka River they were influenced by the operation of a hydropower plant in Brno.

The a and D_{L} values were determined via backward analysis carried out using the advection–dispersion model. The aim was to fit the time series of the modelled concentration values to the concentration values $c(x, t)$ measured in the sampling profiles. The upstream boundary conditions were defined as zero concentration in both rivers. The instantaneous injection of the dye in the Svitava River was specified as a lateral inflow. The initial condition before dye injection was defined as zero concentration of the dye $c\ (x, t_0) = c_0\ (x) = 0$.

The calibration of both models was carried out via the trial and error procedure applied for the studied reaches of the Svitava and Svratka rivers in the direction of flow. The stability of the calculation was controlled by the assessment of Courant and Peclet numbers. The Courant number ranged between 0.4 and 1.0, while the maximum Peclet numbers ranged between 2 and 3, which proved good numerical stability during the simulations.

The dye tests

To determine transport parameters, two dye tests were carried out at the rivers Svratka and Svitava within the territory of the city of Brno, Czech Republic.

Table 1 Empirical equations for D_{L} determination

Author	Empirical equation	
Fischer et al. (1979)	$D_{\mathrm{L}} = 0.011\frac{u^2w^2}{hu^*}$	(11)
Iwasa and Aya (1991)	$D_{\mathrm{L}} = 2.0hu^*\left(\frac{w}{h}\right)^{3/2}$	(12)
Seo and Cheong (1998)	$D_{\mathrm{L}} = 5.915hu^*\left(\frac{w}{h}\right)^{0.62}\left(\frac{u}{u^*}\right)^{1.428}$	(13)
Deng et al. (2001)	$D_{\mathrm{L}} = 0.15\left(\frac{hu^*}{8\varepsilon_T}\right)\left(\frac{w}{h}\right)^{5/3}\left(\frac{u}{u^*}\right)^2$, $\varepsilon_T = 0.145 + \left(\frac{1}{3250}\right)\left(\frac{w}{h}\right)^{1.38}\left(\frac{u}{u^*}\right)$	(14)
Kashefipour and Falconer (2002)	$D_{\mathrm{L}} = 10.612\frac{hu^2}{u^*}$	(15)
Sahay and Dutta (2009)	$D_{\mathrm{L}} = 2.0hu^*\left(\frac{w}{h}\right)^{0.96}\left(\frac{u}{u^*}\right)^{1.25}$	(16)

Table 2 Rearranged empirical equations according to Eq. (20)

Author	D_L relation	
Fischer et al. (1979)	$D_L = 0,011 \frac{Cw^2}{h\sqrt{g}}.u$	(21)
Iwasa and Aya (1991)	$D_L = \frac{2.0h\sqrt{g}}{C}\left(\frac{w}{h}\right)^{3/2}.u$	(22)
Seo and Cheong (1998)	$D_L = 5.915h\frac{\sqrt{g}}{C}\left(\frac{w}{h}\right)^{0.62}\left(\frac{C}{\sqrt{g}}\right)^{1.428}.u$	(23)
Deng et al. (2001)	$D_L = 0.145\left(\frac{h\sqrt{g}}{8\varepsilon_T C}\right)\left(\frac{w}{h}\right)^{5/3}\left(\frac{C}{\sqrt{g}}\right)^{2}.u,\ \varepsilon_T = 0.145 + \left(\frac{1}{3250}\right)\left(\frac{w}{h}\right)^{1.38}\left(\frac{C}{\sqrt{g}}\right)$	(24)
Kashefipour and Falconer (2002)	$D_L = 10.612h\frac{C}{\sqrt{g}}.u$	(25)
Sahay and Dutta (2009)	$D_L = 2.0h\frac{\sqrt{g}}{C}\left(\frac{w}{h}\right)^{0.96}\left(\frac{C}{\sqrt{g}}\right)^{1.25}.u$	(26)

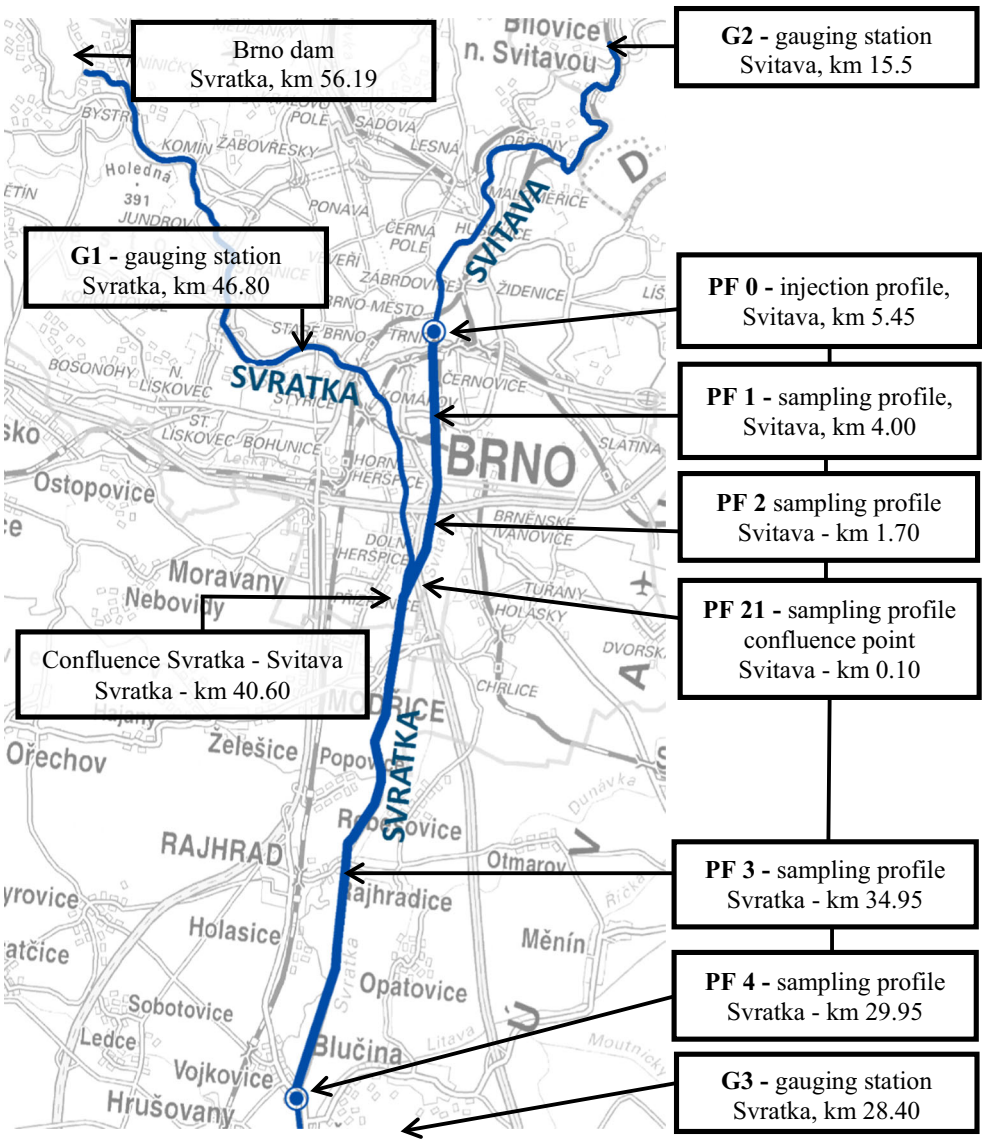

Fig. 1 Schematic diagram of the locality with river reaches of interest marked in bold and with key profiles

Description of the streams and key profiles

The dye tests were carried out on the selected river reaches shown in Fig. 1. They were partly located on the Svitava River between km 0.00 and km 5.45, and partly on the Svratka River between km 29.95 and km 40.60 (the reach downstream of the confluence with the Svitava River). Figure 1 shows a schematic diagram of the rivers of interest and the locations of key profiles (injection and sampling profiles, gauging stations).

The injection profile PF0 was located at stationing km 5.45 on the Svitava River (Table 3).

The dye sampling took place at carefully selected profiles (PF1–PF4). In these profiles rating curves were derived from hydrometric measurements for the estimation of instantaneous discharge during the tests. Along the Svitava River, three sampling profiles were situated at distances of 1.45 (PF1), 3.75 (PF2) and 5.35 km (PF21) from the injection point. (PF21 was added for Test II based on the results of Test I.) Two more profiles were situated along the Svratka River at distances of 11.1 (PF3) and 16.1 km (PF4) from the injection profile (Fig. 1; Table 4).

Sampling profiles were selected that were easily accessible by road and supplied with electric power. It was necessary to ensure that there was enough time to transfer the sampling devices between the profiles. (Only two samplers-fluorometers were available.) Therefore, preliminary numerical analysis of the speed of solute transport in the river was carried out in order to estimate arrival times for the dye front and tail in the predefined profiles.

An important role is played by the way in which the dye is applied to the river, namely the selection of the injection point in a channel cross section. The one-dimensional transport model (Eq. (5)) assumes uniform distribution of tracer concentration at each cross section along the watercourse. However, with point injection uniform tracer concentrations cannot be achieved in a river up to a certain distance from the injection point (mixing length). In medium size rivers, the mixing length can be in the order of hundreds of metres, while in large rivers it can even be dozens of kilometres (Leibundgut et al. 1993).

The locations of sampling profile PF1 (a sampling profile downstream of the injection profile) and PF3 (a sampling profile downstream of the confluence) were defined based on a preliminary assessment of the mixing length according to Fischer et al. (1979), Eq. (27) for the injection in the centre of the channel (Test I) and Fischer et al. (1979), Eq. (28), Sanders and Ward (1978)—Eq. (29) for the side injection (Test II):

$$L_M = 0.1\frac{uw^2}{D_{PH}} \tag{27}$$

$$L_M = 0.4\frac{uw^2}{D_{PH}} \tag{28}$$

$$L_M = \frac{uw^2}{2D_{PH}} \tag{29}$$

The resulting mixing lengths for the injection in the centre of the Svitava River (Test I) and side injection (Test II) are shown in Table 3.

Figure 1 shows the selected sampling profiles, which can be seen to easily satisfy the required distances given in Table 3.

The gauging stations (marked G) are profiles monitored by hydrological services which take continuous measurements of water level and discharge there over the long term. Data from these profiles were available for the calibration of the hydrodynamic model.

The Svitava and Svratka rivers can be characterized as small to medium size rivers. The Svitava River (Fig. 2 left) is a regulated river with a trapezoidal channel which has a bed width of 8–10 m. The reach of interest of the Svratka River (Fig. 2 right) is also mostly regulated with an average riverbed width of 15–20 m.

Table 3 Resulting mixing lengths

River	Profiles	Test I		Test II	
		L_M (m)	Equation	L_M (m)	Equation
Svitava	PF0—PF1	230	(29)	960	(30)
				1200	(31)
Svratka	PF21—PF3	1780	(30)	2110	(30)
		2220	(31)	2640	(31)

Dye injection and sampling

The dye was injected into the Svitava River at profile PF 0. 100 g of Rhodamine WT dye was applied via instantaneous injection in each test (Table 4). Two Turner 10-AU fluorometers were used for the dye sampling. The devices were equipped with flow cells for the onsite measurements. Before each test and at each profile, the fluorometers were calibrated at the site by adjusting the offset, thus eliminating impact of the initial fluorescent concentration in the stream. This was done by comparing the standard Rhodamin WT concentration of 100 mg/l in distilled water with the concentration in the stream.

During the tests, dye concentration was determined automatically over a predefined time interval of 5 s.

Conditions during the tests

In order to obtain a relevant assessment of solute transport, information about geometrical characteristics and instantaneous hydraulic conditions (discharge, mean velocity) is

Table 4 Overview of sampling profiles

PF	Stream	Station (km)	Distance from injection profile (km)	Description of monitoring profile
PF0	Svitava	5.45	0.00	Injection profile—bridge at Krenova Street
				Test I—central injection
				Test II—injection from the right side bank
PF1	Svitava	4.00	1.45	Left bank, concrete wall under a bridge
PF2	Svitava	1.70	3.75	500 m downstream of a road bridge
PF21	Svitava	0.00	5.45	Upstream from the river junction (only Test II)
PF3	Svratka	34.95	11.11	Rajhrad Weir
PF4	Svratka	29.95	16.11	Downstream of a road bridge in the village of Židlochovice

Fig. 2 Svitava River (*left*) and the Svratka River (*right*)

crucial. The data from measurements taken at sampling profiles were combined with data provided by the Czech Hydrometeorological Institute (CHMI) from three nearby gauging stations G1, G2, G3 (Fig. 1). A hydrodynamic analysis was carried out, which involved the calibration of a hydrodynamic model (see Chapter 5) using the following data:

- observed discharges from three gauging stations (G1, G2, G3),
- discharges in profiles PF1 and PF2 based on measured water stages and previously derived rating curves,
- discharges at Rajhrad Weir taken from the weir rating curve.

The discharges in the Svitava River at gauging station G2 were approximately constant for both tests (see Table 5) as the weather conditions during both tests were practically the same. The hydrodynamic conditions in the Svratka River were influenced by the operation of a peak load hydropower plant at Brno Dam, which is located 15.5 km upstream of the junction with the Svitava River. In both the Svitava and Svratka rivers, practically no sediment transport is present due to the numerous weirs and the dam reservoir upstream of the studied reaches.

Results

Backward analysis

The results of the calibration of the hydraulic model (backward analysis) for the Svitava River provided fairly good conformity between observed and calculated discharges and velocities primarily due to the approximately steady-state hydraulic conditions (Table 6). Due to the small amount of observed data (each of the discharge readings taken during the tests was for a 15 min period), rigorous statistical analysis could not be performed for the profiles on the Svitava River. The maximum relative error in discharges in Test I varied from 2 to 11%, and from 0.05 and 6% in Test II. The average absolute errors in the measured and calculated discharges ΔQ and corresponding velocities Δu are shown in Table 7.

No discharge or velocity measurements were taken at the Svratka River in PF3 and PF4. The discharges in the Svratka River were calibrated using data from gauging station G3 and qualitatively from water stages measured at Rajhrad Weir. The upstream boundary condition was set up using data from gauging station G1 upstream of the junction with the Svitava River and calibrated using discharges

Table 5 Flow characteristics of the tracer tests (measured values)

River	Reach no.	River reach	TEST I					TEST II				
			h (m)	w (m)	Q (m^3/s)	u (m/s)	u^* (m/s)	h (m)	w (m)	Q (m^3/s)	u (m/s)	u^* (m/s)
Svitava	1	km 4.0–5.45	0.95	11.5	3.40	0.55	0.058	0.78	10.7	2.10	0.43	0.046
Svitava	2	km 1.7–4.0	1.0	11.7	3.70	0.44	0.051	0.80	10.8	2.18	0.33	0.039
Svitava	3	km 0.0–1.7	1.1	12.0	3.72	0.42	0.049	0.90	11.2	2.20	0.30	0.036
Svratka	4	km 40.61–34.95	1.9	24.0	12.13	0.25	0.026	1.75	23.5	5.90	0.23	0.024
Svratka	5	km 34.95–29.95	0.85	20.0	11.58	0.45	0.046	0.80	19.5	5.95	0.32	0.032

Table 6 Comparison of calculated and measured Q and u values for the Svitava River (PF1, PF2)

Time	PF1				PF2			
	Measured		Calculated		Measured		Calculated	
	Q_m (m^3/s)	u_m (m/s)	Q_c (m^3/s)	u_c (m/s)	Q_m (m^3/s)	u_m (m/s)	Q_c (m^3/s)	u_c (m/s)
Test I								
10:00	3.30	0.55	3.26	0.49	–	–	3.34	0.44
11:00	3.40	0.57	3.27	0.50	3.35	0.43	3.17	0.43
12:00	3.50	0.58	3.58	0.52	3.70	0.44	3.57	0.44
13:00	3.30	0.55	3.28	0.51	3.70	0.44	3.61	0.45
14:00	–	–	3.92	0.57	3.35	0.43	3.15	0.43
15:00	–	–	3.79	0.56	3.35	0.43	3.34	0.44
Test II								
10:00	2.04	0.43	2.04	0.37	–	–	1.91	0.30
11:00	2.18	0.46	2.16	0.38	2.22	0.33	2.09	0.33
12:00	2.24	0.47	2.22	0.39	2.17	0.32	2.19	0.34
13:00	–	–	2.39	0.40	2.12	0.31	2.09	0.33
14:00	–	–	2.35	0.40	2.12	0.31	2.11	0.33
15:00	–	–	2.28	0.39	2.17	0.32	2.20	0.34

Table 7 Average absolute errors in measured and calculated discharges and velocities

River	Profile	TEST I		TEST II	
		ΔQ (m^3/s)	Δu (m/s)	ΔQ (m^3/s)	Δu (m/s)
Svitava	PF1	0.068	0.011	0.013	0.030
Svitava	PF2	0.069	0.004	0.044	0.016

provided by the CHMI for gauging station G3 located close to the downstream end of the model domain.

The efficiency of the hydrological model for the Svratka River was assessed using the Nash–Sutcliffe efficiency coefficient (Nash and Sutcliffe 1970):

$$E_Q = 1 - \frac{\sum_{t=1}^{T}\left(Q_c^t - Q_m^t\right)^2}{\sum_{t=1}^{T}\left(Q_m^t - \bar{Q}_m\right)^2} \quad (30)$$

where Q_c^t is the calculated discharge, Q_m^t is the measured discharge at time t, and $\bar{Q}_m$ is the mean of the measured discharges.

The efficiency coefficients E_Q expressing the agreement of the measured and calculated discharges for the individual tests at gauging station G3 are $E_Q = 0.76$ for Test I and $E_Q = 0.85$ for Test II. It can be seen that the hydrological model provides very good efficiency in both tests (The E value is close to 1).

In the case of the Svratka River, better calibration results were achieved during Test II, where the maximum relative error in the discharge at gauging station G3 did not exceed 5%, while at one point during Test I (at the discharge peak) the error reached even 17% (Fig. 3). These differences may be attributed to uncertainties in the observed discharges, which may be up to 10% (CSN 75 1400 2014), and also could be due to the expected inaccuracy in the numerical solution (Crowder et al. 2004). A minor uncertainty up to 2% may be caused by the estimate of the discharge from the Litava River, a tributary entering the Svratka River between profiles P4 and G3.

The results of the convection–dispersion analysis are expressed by comparing measured and calculated concentrations of the dye at profiles PF1, PF2 and PF21 along the

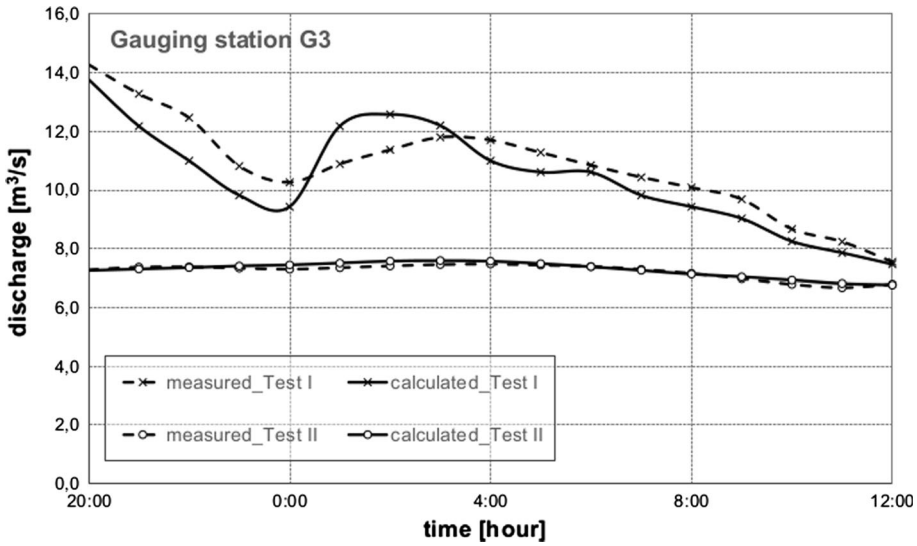

Fig. 3 Comparison of values of Q calculated and measured in the Svratka River at gauging station G3

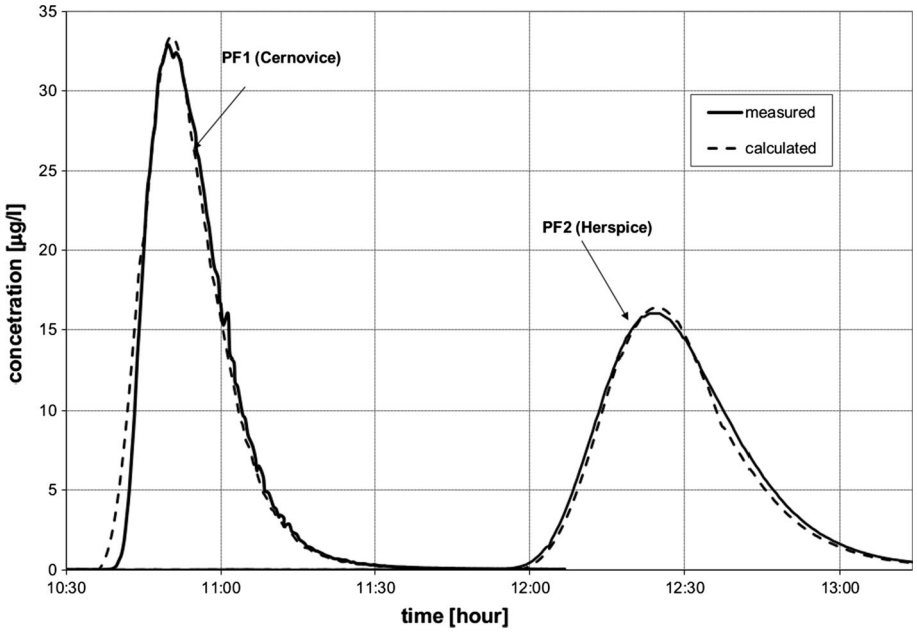

Fig. 4 Comparison of calculated and measured concentrations at the Svitava River in profile PF1 (Test I)

Svitava River (Figs. 4, 5) and PF3 and PF4 along the Svratka River (Figs. 6, 7).

For both tests, relatively good agreement was achieved in all sampling profiles located along the Svitava River (Figs. 4, 5). This was due to the relatively stable discharge there, and also to the regular geometry of the river (Fig. 2 left). Profile PF21 was added for the second test in order to get a better description of dye transport in the Svitava River close to the junction with the Svratka River.

A comparison of the measured and calculated concentrations of the dye at profiles PF3 and PF4 along the Svratka River (Figs. 6, 7) shows much greater differences namely in the arrival time of the front of the dye cloud. Much better agreement was achieved with regard to the peak concentration and its arrival time.

The efficiency of the transport model was assessed using the Nash–Sutcliffe efficiency coefficient (Eq. (30)), modified for concentrations:

$$E_c = 1 - \frac{\sum_{t=1}^{T} \left(c_c^t - c_m^t\right)^2}{\sum_{t=1}^{T} \left(c_m^t - \bar{c}_m\right)^2} \tag{31}$$

Corresponding efficiency coefficients E_c are shown in Table 8, which shows quite good agreement in all sampling profiles for both tests (efficiency coefficient E_c value is between 0.3 and 1).

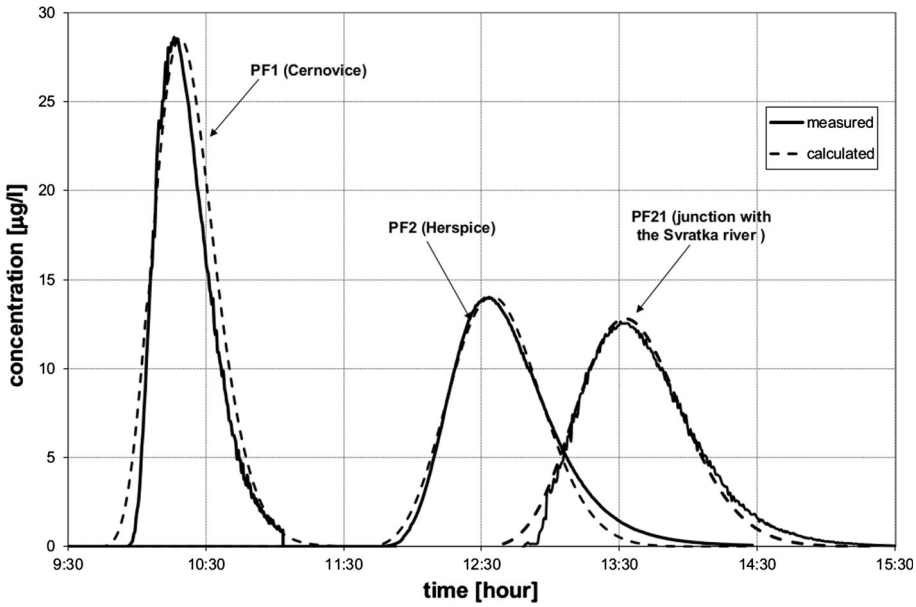

Fig. 5 Comparison of calculated and measured concentrations at the Svitava River (Test II)

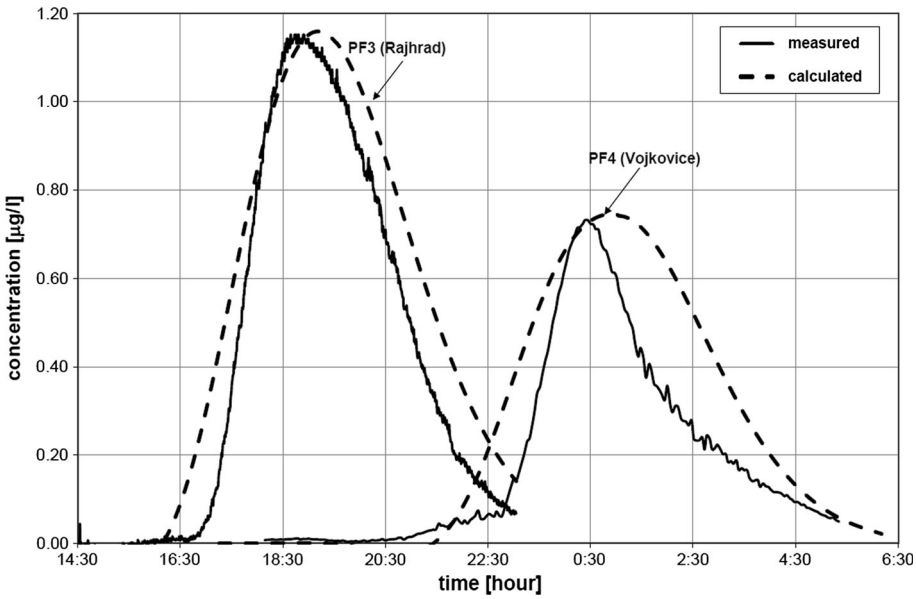

Fig. 6 Comparison of calculated and measured concentrations at the Svratka River (Test I)

The differences between the measured and calculated concentrations can be attributed to following facts:

- The calibration of the hydrological model produced certain inaccuracies (see the discussion above) namely due to the much more unstable hydrodynamic conditions present in the Svratka River during Test I (Fig. 3).
- The assumption of constant concentration in the stream cross section was not fully fulfilled both in the Svitava River (Fig. 8) and also in the Svratka River namely downstream of the junction with the Svitava River.
- A significant role is played by the location of the sampling probe in the sampling profile, namely in the case of wider channels. In the event of unsteady flow, the main transport path may change and temporarily miss the probe. This is probably the main reason for the certain lack of total dye mass in the Svratka River during Test I and partly also at PF3 during Test II.
- Some adsorption of the dye on the material of the river bed and banks was identified. The mass balance assessed from the sampling data showed that the measured dye mass was smaller by several per cent when compared with the injected amount. However, this finding advocates the assumption that the dye tracer exhibits fairly conservative behaviour.
- In profile PF 4 during Test II (period 10:00—11:00), a measurement error occurred when a probe became clogged with algae (Fig. 7).

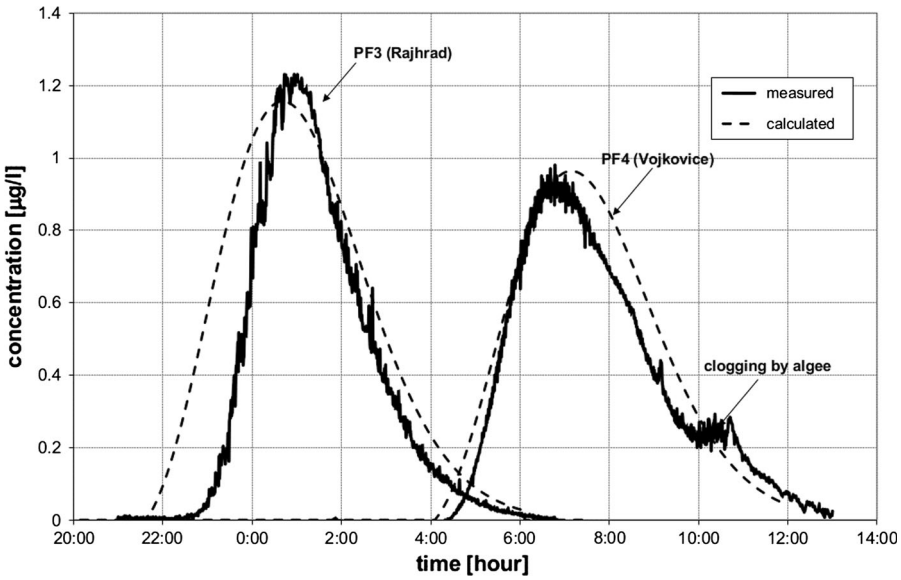

Fig. 7 Comparison of calculated and measured concentrations at the Svratka River (Test II)

Table 8 Nash-Sutcliffe efficiency coefficient E_c for the transport model

River	Profile	TEST I	TEST II
Svitava	PF1	0.31	0.92
Svitava	PF2	0.33	0.98
Svitava	PF21	–	0.98
Svratka	PF3	0.90	0.70
Svratka	PF4	0.31	0.94

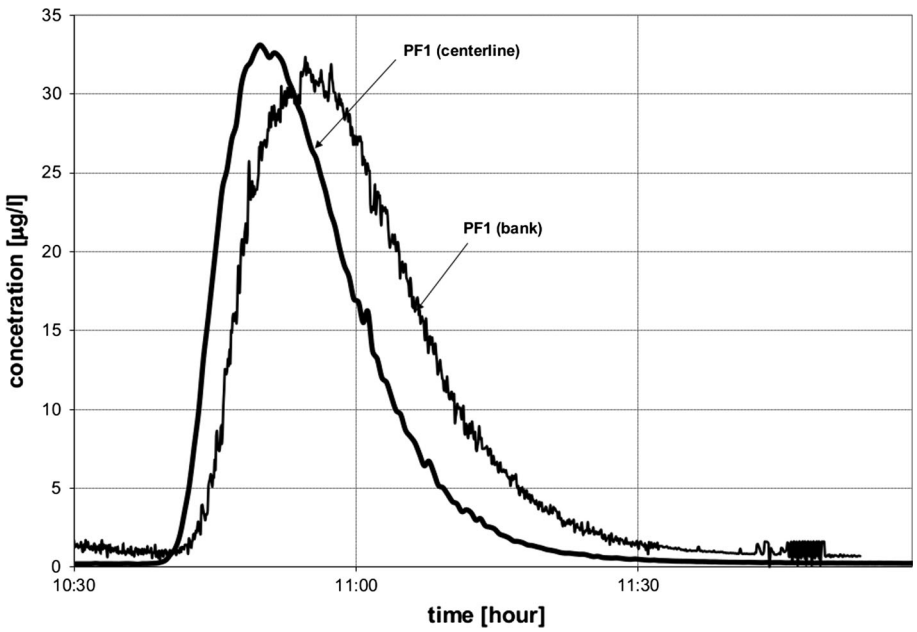

Fig. 8 Concentration in cross-sectional PF1 at the centreline and close to the bank during Test I

During Test I, the assumed condition of constant concentration in the cross section was verified at PF1 in the Svitava River. The verification was carried out via parallel sampling by two probes located at the river centreline and at the left bank. Slightly faster transport was observed at the centreline. The peak of dye concentration at the

Table 9 Resulting dispersion factor a and longitudinal dispersion coefficient D_L

	Reach no.		Distance from injection point [km]	Test I		Test II	
				a (m)	D_L (m^2/s)	a (m)	D_L (m^2/s)
Svitava	1	km 4.00–5.45	0.0–1.45	14.9	8.2	16.7	7.4
	2	km 1.70–4.00	1.45–3.75	19.1	8.4	21.2	7.5
	3	km 0.00–1.70	3.75–5.45	18.6	7.8	23.0	7.2
Svratka	4	km 40.61–34.95	5.45–10.11	32.0	8.0	28.6	7.2
	5	km 34.95–29.95	10.11–16.11	21.1	9.5	26.2	8.3

Reach km 40.61–34.95 at the Svratka River represents the Rajhrad Weir basin

Table 10 Resulting dispersion factor a and longitudinal dispersion coefficient D_L according to Eqs. (21)–(26)

	Reach no.	Equation (21)		Equation (22)		Equation (23)		Equation (24)		Equation (25)		Equation (26)	
		a	D_L	a	D_L	a	D_L	a	D_L	a	D_L	a	D_L
Test I													
Svitava	1	14.4	7.9	8.5	4.7	68.9	37.9	44.0	24.2	95.0	52.2	36.5	20.1
	2	12.9	5.7	9.3	4.1	68.2	30.0	41.9	18.5	91.1	40.1	36.3	16.0
	3	12.4	5.2	9.2	3.9	71.8	30.2	42.4	17.8	100.2	42.1	37.3	15.7
Svratka	4	31.7	7.9	18.0	4.5	141.9	35.5	92.7	23.2	191.5	47.9	76.1	19.0
	5	50.3	22.6	20.0	9.0	94.3	42.4	76.4	34.4	87.7	39.5	62.2	28.0
Test II													
Svitava	1	15.0	6.4	8.5	3.7	60.7	26.1	41.1	17.7	76.9	33.1	33.6	14.5
	2	13.6	4.5	9.4	3.1	59.3	19.6	39.3	13.0	72.0	23.8	33.2	11.0
	3	12.7	3.8	9.5	2.9	62.9	18.9	39.7	11.9	79.3	23.8	34.4	10.3
Svratka	4	33.4	7.7	17.9	4.1	136.5	31.4	92.0	21.2	178.8	41.1	74.6	17.2
	5	50.9	16.3	19.8	6.3	90.8	29.0	74.0	23.7	82.6	26.4	60.6	19.4

centreline arrived about 7 min before the peak at the left bank. The peak concentration at the centreline was about 3% higher than at the bank (Fig. 8). The non-zero offset at the curve corresponding to the channel bank was caused by technical problems that affected the measurement device; algae at the bank became stuck to the probe. This was also probably the reason for the concentration fluctuations (see also Fig. 7).

Longitudinal dispersion characteristics

First, the longitudinal dispersion characteristics a and D_L (Eq. (20)) were derived by backward analysis (Backward analysis and Backward analysis in sections) using data from the two dye tests. The resulting values for the river reaches displayed in Table 5 are shown in Table 9, where the mean values along the reaches between the sampling profiles are shown. Secondly, the obtained parameters a and D_L were compared with those obtained from empirical formulas Eqs. (21)–(26) derived using experimental research by various authors and based on dimensional analysis. When comparing Eqs. (21)–(26) with Eq. (20), it can be seen that parameter a expresses the geometrical and frictional parameters of the channel, while the channel hydraulics is expressed by flow velocity u.

The values obtained for dispersion factor a are proportional to the average water depth h, channel width w and shear velocity u^*. In the Svitava River the resulting values for a varied between 14.9 and 18.6 m for Test I and from 16.7 to 23.0 m for Test II. Generally, higher values of a correspond to lower discharge in reaches 1, 2, 3 and 5. This caused a decrease in parameter w/h in these reaches, which have almost vertical banks and low water depth (see Fig. 2 left). In the case of reach 4 at the Svratka River, which corresponds to the weir backwater, w/h remains approximately stable and the value of a is governed by the increase in water depth only. Along this reach a has the highest value due to the lower hydraulic losses at the weir pool.

Derived values of D_L for the Svitava River varied between 7.8 and 8.4 m^2/s during Test I and between 7.2 and 7.5 m^2/s during Test II. The slightly higher dispersion coefficients obtained in Test I correspond to higher discharges and velocities during this test (Table 5). For the

Svratka River, the longitudinal dispersion values were lower within the reach between km 34.95 and 40.61. This was caused by the influence of significantly lower velocities in the Rajhrad Weir backwater. The derived values of D_L were 8.0 and 7.2 m^2/s for Test I and II, respectively. In the last reach between PF3 and PF4, the resulting D_L values were 9.5 m^2/s for Test I and 8.3 m^2/s for Test II. The lower D_L values obtained during Test II are also due to the lower discharges and velocities that occurred.

In Tables 10, 11 and 12; Figs. 9 and 10, resulting a and D_L are compared with values obtained from empirical formulas Eqs. (21)–(26). The comparison shows generally good agreement with the a and D_L values obtained by the backward analysis of the dye tests, especially in the case of

Table 11 Ratios between the experimentally obtained values for a and D_L and those computed using Eqs. (21)–(26)

	Reach no.	Equation (21)	Equation (22)	Equation (23)	Equation (24)	Equation (25)	Equation (26)
Test I							
Svitava	1	0.97	0.57	4.62	2.95	6.37	2.45
	2	0.7	0.5	3.6	2.3	5.0	1.9
	3	0.7	0.5	3.9	2.4	5.7	2.0
Svratka	4	1.0	0.5	4.5	3.0	6.2	2.4
	5	2.4	0.9	4.5	3.6	4.2	2.9
Test II							
Svitava	1	0.87	0.50	3.53	2.39	4.47	1.96
	2	0.6	0.4	2.6	1.7	3.2	1.5
	3	0.5	0.4	2.6	1.7	3.3	1.4
Svratka	4	1.1	0.6	4.4	2.9	5.7	2.4
	5	2.0	0.8	3.5	2.9	3.2	2.3

Table 12 Comparison of the obtained results with other studies

Author	Channel	h (m)	w (m)	u (m/s)	u^* (m/s)	D_L (m^2/s)
Godfrey and Frederick (1963)	The Clinch River	0.58	36	0.3	0.049	8.1
Seo and Cheong (1998)	Antietam Creek	0.39	15.8	0.32	0.06	9.3
	Copper Creek	0.49	16.2	0.25	0.079	9.5
Tayfur and Singh (2005)	Bayou Anacoco	0.45	17.5	0.32	0.024	5.8
	The Comite River	0.26	13.0	0.31	0.044	7.0
	The Tickfaw River	0.59	15.0	0.27	0.080	10.3

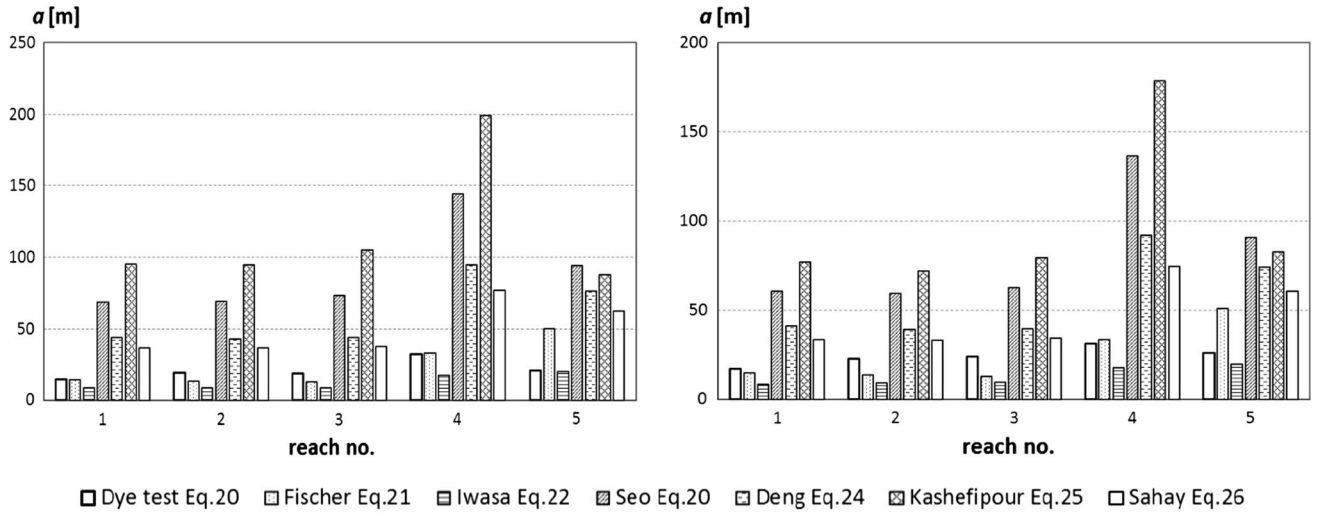

Fig. 9 Comparison of dispersion factor a: Test I—left, Test II—right

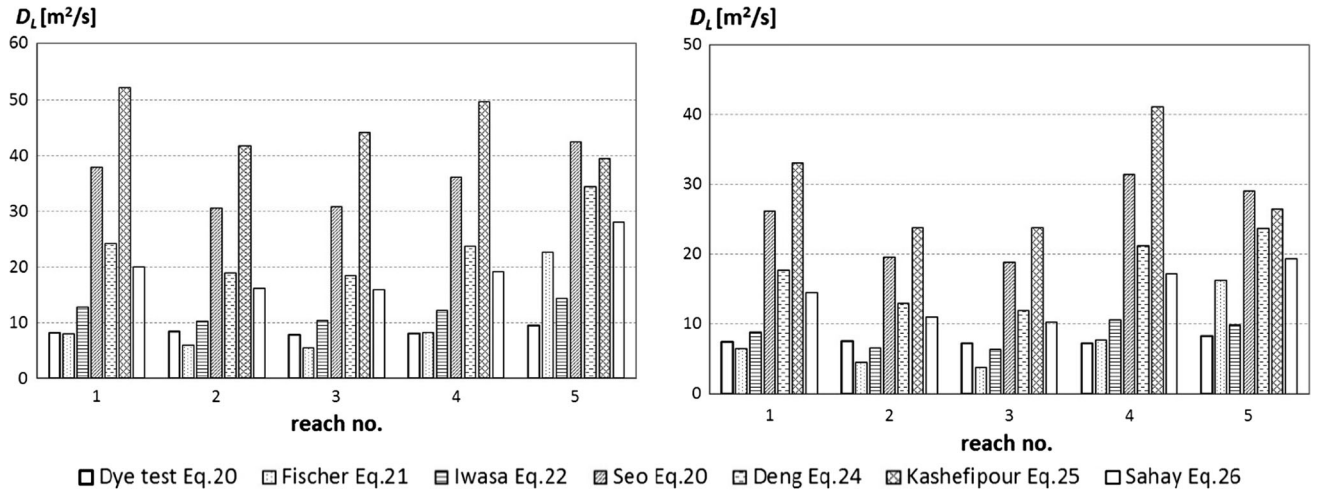

Fig. 10 Comparison of longitudinal dispersion coefficient D_L: Test I—left, Test II—right

Eq. (22), where the relative error for all reaches is smaller than 56%. In reaches 1–4, the best agreement was provided by Eq. (21), which provides an error of less than 30%. In the case of reach 5, the dispersion coefficient is overestimated by 40% due to the dominant effect of channel width in Eq. (21). The remaining equations overestimate both a and D_L several times (see Table 11; Figs. 9 and 10).

The resulting D_L values were also compared with other earlier published studies with similar open channel and flow parameters. It can be seen that the D_L values obtained in this study (Table 9) are similar to the values in Table 12.

Conclusions

The paper deals with the evaluation of dye tests performed in the Svitava and Svratka rivers. Two dye tests (Test I, Test II) were carried out at a 16.1-km-long reach with 4 sampling profiles used for Test I and 5 profiles for Test II. Backward analysis was performed using a one-dimensional unsteady transport model via its calibration for the dye test data. The conformity of the modelled results with the measured data was very good for the Svitava River. Certain differences between the modelled and measured dye concentration values and also total mass appeared in profiles PF3 and PF4 in the Svratka River where the model calibration was more complicated due to unsteady hydraulic conditions during Test I in particular. However, the achieved results might be considered acceptable with respect to the adopted simplifications and uncertainties.

The values of longitudinal dispersion characteristics a and D_L derived from the transport-dispersion model were compared with the results of empirical formulas. The best fit was provided by Eq. (21) (Fischer et al. 1979) and Eq. (22) (Iwasa and Aya 1991), for which the relative error was mostly less than 50%. The longitudinal dispersion coefficients obtained in this study range between $D_L = 7.2$ and 9.5 m^2/s and correspond well with values obtained by older studies (Table 12).

The mass balance of injected dye (100 g) showed the good agreement obtained for the dye mass that passed through profiles PF1, PF2 and PF21 in the Svitava River. The error was less than 1% of the total injected mass. This corresponds well with the assumption that conservative behaviour would be exhibited by the dye tracer. The more significant drop in total dye mass in PF3 and PF4 during Test I was caused by the location of the sampling probe.

The values of the dispersion parameters are characteristic for small and medium channels with the above-described parameters. The study provides some guidance to MIKE11 users concerning the determination of appropriate values of dispersion factor $\underline{a}$ using channel characteristics.

Acknowledgements This paper has been prepared under project No. LO1408: AdMaS UP—Advanced Materials, Structures and Technologies, and project FAST-S-16-3655: Tools for the risk assessment of surface water quality under extreme hydrological situations.

References

Abbot MB, Cunge JA (1982) Engineering applications of computational hydraulics, vol 1. Pitman Advanced Publishing Program, Boston

Ambrose RB, Barnwell TO, McCutcheon SC, Williams JR (1994) Computer models for water quality analysis. McGraw-Hill, New York

Ani E-C, Wallis S, Kraslawski A, Agachi PS (2009) Development, calibration and evaluation of two mathematical models for pollutant transport in a small river. Environ Model Softw 24:1139–1152

Azamathulla HMd, Wu FC (2011) Support vector machine approach for longitudinal dispersion coefficients in natural streams. Appl Soft Comput J. doi:10.1016/j.asoc.2010.11.026

Boxall JB, Guymer I (2007) Longitudinal mixing in meandering channels: new experimental data set and verification of a predictive technique. Water Res 41:341–354

Brown LC, Barnwell TO (1987) The enhanced stream water quality models. QUAL2E. QUAL2E—UNCAS—documentation and user manual. Athens. USA. p 188

Crabtree B, Earp W, Whalley P (1996) A demonstration of the benefits of integrated wastewater planning for controlling transient pollution. Water Sci Technol 33(2):209–218

Crowder RA, Pepper AT, Whitlow C, Sleigh A, Wright N, Tomlin C (2004) Benchmarking hydraulic river modelling software packages. R&D Technical Report. Defra/Environment Agency. Great Britain. p 40

CSN 75 1400 (2014) Hydrological data of surface waters. Czech National Standard. p 23

Daněček J, Ryl T, Říha J (2002) Determination of longitudinal hydrodynamic dispersion in water courses with solution of Fischer's integral. J Hydrol Hydromech 50(2):104–113

Deng ZQ, Singh VP, Bengtsson L (2001) Longitudinal dispersion coefficient in straight rivers. J Hydraul Eng 127(11):919–927

DHI (2016) MIKE 11 reference manual. Danish Hydraulic Institute, Hørsholm

Feuerstein DL, Selleck RE (1963) Fluorescent tracers for dispersion measurement. J Sanit Eng Div 89(4):1–22

Field M (2003) Tracer-test planning using the efficient hydrologic tracer-test design (EHTD) program 2005. U.S. Environmental Protection Agency. Washington DC, EPA/600/R-03/034B, 2003

Fischer HB (1967) Analytical predictions of longitudinal dispersion coefficient in natural streams. In: Proceedings of the twelfth international association for highway research congress, vol 4, Part 1

Fischer HB, List J, Koh C, Imberger J, Brooks NH (1979) Mixing in inland and coastal waters. Academic Press, New York, p 483

Flury M, Wai NN (2003) Dyes as tracers for vadose zone hydrology. Rev Geophys 41(1):2-1–2-37

Fourier J (1822) Théorie analytique de la chaleur. (The analytical theory of heat). Paris: Firmin Didot Père et Fils. p 639

Godfrey RG, Frederick BJ (1963) Dispersion in natural streams. U.S. G.S. report

HEC-RAS (2016) Hydrologic Engineering Center's River Analysis System. USACE. http://www.hec.usace.army.mil (last access: 10 July 2017)

Iwasa Y, Aya S (1991) Predicting longitudinal dispersion coefficient in open-channel flows. In: Proceedings of international symposium on environmental hydraulics, Hong Kong, pp 505–510

Jain SC (2000) Open-channel flow. Wiley, New York, p 328

Kashefipour MS, Falconer RA (2002) Longitudinal dispersion coefficients in natural channels. Water Resour Res 36(6):1596–1608

Kim D (2012) Assessment of longitudinal dispersion coefficients using acoustic doppler current profilers in large river. J Hydro Environ Res 6:29–39

Knopman DS, Voss CI (1987) Behaviour of sensitivities in the one-dimensional advection-dispersion equation: implications for parameter estimation and sampling design. Water Resour Res 23:253–272

Leibundgut CH, Speidel U, Wiesner H (1993) Transport processes in rivers investigated by tracer experiments. Tracers in hydrology. In: Proceedings of the Yokohama symposium. July, 1993

Liu H (1977) Predicting dispersion coefficient of streams. J Environ Eng Div 103(1):59–69

Martin JL, McCutcheon SC, Schottman RW (1999) Hydrodynamics and transport for water quality modeling. Lewis Publishers, Boca Raton, p 795

McCutcheon SC (1989) Water quality modelling. Vol. I. Transport and surface exchanges in rivers. CRC Press, Boca Raton, pp 103–110

Murphy E, Ghisalberti M, Nepf H (2007) Model and laboratory study of dispersion in flows with submerged vegetation. Water Resour 43(5)

Nash JE, Sutcliffe JV (1970) River flow forecasting through conceptual models part I—A discussion of principles. J Hydrol 10(3):282–290

Perucca E, Camporeale C, Ridolfi L (2009) Estimation of the dispersion coefficient in rivers with riparian zone. Adv Water Resour 32:78–87

Pujol LI, Sanchez-Cabeza JA (1999) Determination of longitudinal dispersion coefficient and velocity of the Ebro river waters (Northeast Spain) using tritium as a radiotracer. J Environ Radioact 45:39–57

Riahi-Madvar H, Ayyoubzadeh SA, Khadangi E, Ebadzadeh MM (2009) An expert system for predicting longitudinal dispersion coefficient in natural streams by using ANFIS. Expert Syst Appl 36:8589–8596

Sahay RR (2011) Prediction of longitudinal dispersion coefficients in natural rivers using artificial neural network. Environ Fluid Mech 11:544–552

Sahay RR (2013) Predicting longitudinal dispersion coefficients in sinuous rivers by genetic algorithm. J Hydrol Hydromech 61 (3):214–221

Sahay RR, Dutta S (2009) Prediction of longitudinal dispersion coefficients in natural rivers using genetic algorithm. Hydrol Res 40(6):544

Sanders TG, Ward RC (1978) Relating stream standards to regulatory water quality monitoring practices. In: Proceedings of the American water resources association symposium on establishment of water quality monitoring programs

Seo IW, Cheong TS (1998) Predicting longitudinal dispersion coefficient in natural streams. J Hydraul Eng 124(1):25–32

Tayfur G, Singh VP (2005) Predicting longitudinal dispersion coefficient in natural streams by artificial neural networks. J Hydraul Eng 131(11):991–1000

Tealdi S, Camporeale C, Perruca R (2010) Longitudinal dispersion in vegetated rivers with stochastic flows. Adv Water Resour 33:562–571

Toprak ZF, Sen Z, Savci ME (2004) Comment on "Longitudinal dispersion coefficients in natural channels". Water Res 38:3139–3143

USEPA (1989) Exposure Factors Handbook. U.S. Environmental Protection Agency. Office of Health and Environmental Assessment. EPA/600/8-89/043. Washington

Van Genuchten MT, Alves WJ (1982) Analytical solutions of the one-dimensional convective-dispersive solute transport equation. Technical Bulletin No. 1661. United States Department of Agriculture. Washington

Van Mazijk A (1996) One-dimensional approach of transport phenomena of dissolved matter in rivers. Communication on hydraulic and geotechnical engineering. FCE TU Delft. Report No. 96-3, p 310

Van Mazijk A, Veling EJM (2005) Tracer experiments in the Rhine Basin: evaluation of the skewness of observed concentration distributions. J Hydrol 307:60–78

Veliskova Y, Kohutiar J (1992) Two-dimensional model of dispersion in natural channels. J Hydrol Hydromech 40(5):409–424

Yotsukura N, Fiering MB (1964) Numerical solution to a dispersion equation. J Hydraulics Div 90(5):83–104